THE JOURNAL OF BIOLOGICAL CHEMISTRY VOL. 284, NO. 31, pp. 20638–20648, July 31, 2009

Thrombin Promotes Release of ATP from Lung Epithelial Cells through Coordinated Activation of Rho- and Ca^{2+}-dependent Signaling Pathways*[S]

Received for publication, December 19, 2008, and in revised form, April 6, 2009 Published, JBC Papers in Press, May 12, 2009, DOI 10.1074/jbc.M109.004762

Lucia Seminario-Vidal[‡], Silvia Kreda[§], Lisa Jones[§], Wanda O'Neal[§], JoAnn Trejo[¶], Richard C. Boucher[§], and Eduardo R. Lazarowski[§1]

From the Departments of [‡]Cell and Molecular Physiology and [§]Medicine, University of North Carolina, Chapel Hill, North Carolina 27599 and the [¶]Department of Pharmacology, University of California, San Diego, La Jolla, California 92093

Extracellular ATP controls key aspects of lung function via activation of epithelial cell purinergic receptors, but how ATP is released from cells remains poorly understood. To identify mechanistic components upstream of ATP release, we examined the effect of selected G protein coupled-receptor activation on ATP release from lung epithelial cells. The protease-activated receptor (PAR) agonist thrombin elicited a rapid Ca^{2+}-dependent release of ATP from A549 cells. In contrast, the $P2Y_2$ receptor agonist UTP caused negligible ATP release, despite promoting a robust Ca^{2+} response. Agonist-elicited ATP release was associated with Rho activation and was reduced in cells transfected with dominant negative mutants of p115-Rho GEF or RhoA, and by inhibitors of Rho kinase (ROCK). However, RhoA activation alone did not promote ATP release if temporally separated from Ca^{2+} mobilization. PAR3 was the only PAR subtype detected in A549 cells by reverse transcription-PCR. Transfection of cells with human PAR3 cDNA increased thrombin-promoted ATP release, inositol phosphate formation, and RhoA activation. Conversely, small interference RNA against PAR3 diminished thrombin-evoked responses. Thrombin-elicited ATP release was accompanied by an enhanced cellular uptake of propidium iodide in a Ca^{2+}- and ROCK-dependent manner and was inhibited by connexin/pannexin hemichannel blockers. Our data suggest that thrombin promotes ATP release from A549 cells via Rho- and Ca^{2+}-dependent activation of connexin/pannexin hemichannels. The relevance of these findings is highlighted by the observation that exposure of primary cultures of well differentiated human bronchial epithelial cells to thrombin resulted in robust ATP release, which was inhibited by ROCK inhibitors and by connexin/pannexin hemichannel blockers.

Nucleotides and nucleosides within the airway surface liquid regulate mucociliary clearance activities, the primary innate defense mechanism that removes foreign particles and pathogens from the airways (1–4). ATP activates the G_q-coupled $P2Y_2$ receptor ($P2Y_2$-R)[2] present on the airway epithelial cell surface, promoting mucin secretion and ciliary beat frequency, and inhibiting the epithelial Na^+ channel (4–10). In addition, ATP induces activation of a Ca^{2+}-activated Cl^- channel, via $P2Y_2$-R and, possibly, the ATP-gated ion channel $P2X_4$-R (11–13). Adenosine, generated from the hydrolysis of ATP in airway surface liquid, activates the G_s-coupled A_{2b} receptor, promoting cAMP-regulated cystic fibrosis transmembrane conductance regulator Cl^- channel activity (14) and increasing cilia beat frequency (5). In the distal lung, ATP and/or adenosine (mainly via $P2Y_2$-R and A_{2b} receptor, respectively) stimulate type II cell surfactant secretion (15), regulate alveolar ion transport and fluid clearance (16), and contribute to alveolar remodeling and inflammation (17, 18). Although it is recognized that ATP and adenosine are naturally occurring extracellular signals that regulate key physiological components of lung function (1, 19), the origin of these signals in the extracellular milieu is poorly understood.

Lung epithelia exhibit a complex cellular composition, and thus, several mechanisms and pathways likely are involved in the release of nucleotides into the airways and bronchoalveolar space. Circumstantial evidence supports the involvement of both secretory pathways and plasma membrane channels or transporters in the cellular release of nucleotides from non-excitatory tissues. However, unambiguous evidence for either vesicular or conductive/transport mechanisms in the airways and in most non-neural tissues is lacking. Moreover, the regulatory processes involved in ATP release are largely unknown (20).

Although most studies with airway- or alveolar-derived epithelial cells have relied on the use of mechanical and/or osmotic stimuli to promote ATP release, biochemical signals regulating ATP release are less well defined. Recent data suggest that ATP release in hypotonically swollen lung epithelial A549 cells depends on the availability of intracellular Ca^{2+} (21–23). How-

* This work was supported, in whole or in part, by National Institutes of Health Grant P01-HL034322. This work was also supported by Cystic Fibrosis Foundation Grant CFF-SEMINA08FO (to L. S. V.).

[S] The on-line version of this article (available at http://www.jbc.org) contains supplemental Fig. S1.

[1] To whom correspondence should be addressed: Cystic Fibrosis/Pulmonary Research and Treatment Center, 7017 Thurston-Bowles Bldg., CB 7248, University of North Carolina, Chapel Hill, NC 27599-7248. Tel.: 919-966-0991; Fax: 919-966-5178; E-mail: eduardo_lazarowski@med.unc.edu.

[2] The abbreviations used are: $P2Y_2$-R, $P2Y_2$ receptor; PAR, protease-activated receptor; GEF, guanine nucleotide exchange factor; BAPTA-AM, 1,2-bis(*o*-aminophenoxy)ethane-*N*,*N*,*N*′,*N*′-tetraacetic acid (acetoxymethyl ester); $\beta\gamma$-metATP, β,γ-methylene ATP; GPCR, G protein-coupled receptor; siRNA, small interference RNA; ROCK, Rho-associated coiled-coil-containing protein kinase; MLC, myosin light chain; MLCK, MLC kinase; ebselen, 2-phenyl-1,2-benzisoselenazol-3(2H)-one; HBE, human bronchial epithelial; UNC, University of North Carolina; S.A., specific activity; HBSS, Hanks' balanced salt solution; RT, reverse transcription; HA, hemagglutinin.

ever, Ca^{2+}-mobilizing agents (*e.g.* ionomycin and UTP) promoted only minor release of ATP from these cells, relative to hypotonic shock (22, 23), suggesting that signals in addition to Ca^{2+} are required upstream of ATP release. This conclusion was not restricted to epithelial cells. For example, studies from our laboratory and those of others illustrated that Ca^{2+} is necessary but not sufficient to impart maximal ATP release from 1321N1 human astrocytoma cells (24, 25). In these cells, the serine-protease thrombin promote robust Ca^{2+}-dependent nucleotide release via protease-activated receptor-1 (PAR1), and recent evidence indicates that Rho signaling is involved in this response (26).

Because thrombin receptors are expressed in lung epithelial cells (27), we reasoned that PAR activation might physiologically mediate regulated ATP release from these cells. In the present study, we demonstrated that thrombin promotes robust release of ATP from A549 lung epithelial cells via PAR3 activation. We also investigated signaling mechanisms and pathways involved in thrombin-evoked ATP release from A549 cells as well as from physiologically relevant primary cultures of well differentiated human bronchial epithelial (HBE) cells.

EXPERIMENTAL PROCEDURES

Reagents—Human α-thrombin was purchased from Enzyme Research Laboratories (South Bend, IN). 2-Phenyl-1,2-benzisoselenazol-3(2H)-one (ebselen), β,γ-methylene ATP (β,γ-metATP), arachidonylethanolamide, flufenamic acid, carbenoxolone, and luciferase from *Photinus pyralis* were obtained from Sigma. Fura-2-acetoxymethyl ester, 1,2-bis(*o*-aminophenoxy)ethane-*N*,*N*,*N*′,*N*′-tetraacetic acid-acetoxymethyl ester (BAPTA-AM), and thapsigargin were purchased from Molecular Probes (Eugene, OR). Luciferin was obtained from BD Pharmingen (Franklin Lakes, NJ). The Rho Activation Assay Biochem Kit was purchased from Cytoskeleton (Denver, CO). Propidium iodide was purchased from Invitrogen. The PAR1-activating peptide TFLLRNPNDK-amide and the PAR4-activating peptide AYPGKF-amide, respectively (hereafter referred to as PAR1AP and PAR4AP, respectively) were synthesized at the University of North Carolina (UNC) Microprotein Sequencing and Peptide Synthesis Facility. *myo*-[^{3}H]Inositol (20 Ci/mmol) was obtained from Amersham Biosciences. Other chemicals were from sources reported previously (1, 25).

Cell Culture—A549 lung epithelial cells were obtained from the UNC Tissue Culture Facility and grown to confluence in Dulbecco's modified Eagle's medium supplemented with 10% calf serum (HyClone, Ogden, UT), 60 μg/ml (100 IU/ml) penicillin, and 100 μg/ml streptomycin (Invitrogen). Cells were grown on 35-mm plastic dishes for real-time ATP measurements and on 24-well plastic plates for off-line ATP assays, cAMP formation, and inositol phosphate measurements. RhoA pulldown assays and confocal microscopy studies were performed with cells grown on 100-mm Falcon plastic dishes and 8-well Lab-Tek II glass chamber slides (Nalge Nunc Int., Naperville, IL), respectively. Because a gradual decline in thrombin-promoted responses was noted with passages, A549 cells were used within passages 3–14. Polarized cultures of well differentiated primary HBE cells (provided by the UNC Cystic Fibrosis Center Center Tissue Culture Core Lab) were grown on 12-mm Transwell supports (Costar) and maintained at an air-liquid interface that mimics the *in vivo* environment of the airway epithelia, as previously described (1, 28).

Measurement of ATP Release and Hydrolysis—A549 ells were washed twice with Hanks' balanced salt solution (HBSS) supplemented with 1.6 mM $CaCl_2$, 1.6 mM $MgCl_2$, and 25 mM HEPES, pH 7.4 (HBSS+), and incubated for 1 h at 37 °C in HBSS+. For real-time ATP measurements in thin film (Fig. 1*B*), cultures were transferred to a Turner TD-20/20 luminometer (Turner Biosystems, Sunnyvale, CA). Luciferase (15–30 × 10^6 light units mg^{-1}) and luciferin (60 μM) were added, and luminescence was monitored, as previously described (28). Off-line ATP measurements were performed via a LB953 AutoLumat luminometer (Berthold), as previously described (29). Calibration curves using known concentrations of ATP were generated at the end of each experiment. None of the reagents used during ATP release measurements interfered with the luciferase reaction. To assess ATP hydrolysis, 100 nM ATP was added to cells in the absence or presence of 30 μM ebselen and 300 μM β,γ-metATP, two previously characterized ATP hydrolysis inhibitors (28–31). Samples were collected at various times, and the resulting ATP concentration was measured as indicated above. Primary HBE cells were rinsed and incubated with 300 μl of mucosal and 500 μl of basolateral HBSS (1), and ATP release was measured off-line, as described above.

Inositol Phosphate Formation—A549 cells were labeled overnight in inositol-free Dulbecco's modified Eagle's medium containing 2 μCi/ml *myo*-[^{3}H]inositol (S.A., 20 Ci/mmol). Primary HBE cells were labeled for 3 days in 500 μl of basolateral and 100 μl of mucosal medium containing 10 μCi/ml *myo*-[^{3}H]inositol. At the time of assay, 10 mM LiCl was added to the cells for 10 min, followed by 20-min incubation in the presence of drugs. Incubations were terminated by the addition of 0.75 ml of 50 mM formic acid and 0.25 ml of 150 mM ammonium hydroxide. [^{3}H]Inositol phosphates were separated on Dowex anion-exchange columns and quantified as previously described (32).

Calcium Mobilization—A549 cells grown on glass coverslips were loaded with Fura-2-acetoxymethyl ester for 30 min. Cells were washed and mounted on a platform of a fluorometer-coupled microscope, and fluorescence from 30–40 cells was acquired alternately at 340 and 380 nm. Other details were as previously described (28).

cAMP Quantification—Cells were rinsed, preincubated for 10 min in HBSS containing 200 μM 3-isobutyl-1-methylxanthine, and subsequently challenged for an additional 10 min with 30 μM forskolin and the indicated concentration of thrombin. The conversion of ATP to cAMP was quantified by high-performance liquid chromatographic analysis of 1,N^6-ethenoadenine derivatives, as previously described (1).

RT-PCR Analysis—Total RNA was prepared using the RNeasy Mini Kit (Qiagen) and reverse-transcribed using SuperScript III reverse transcriptase (RT, Invitrogen). RT-PCR was performed using the following cycling conditions: 4 min/94 °C, 1 min/72 °C, 45 s/94 °C, 1 min/55 °C, and 1 min/72 °C; 36 cycles. PAR1 (GenBank™ M62424), PAR2 (GenBank™ U34038), PAR3 (GenBank™ U92972), and PAR4 (GenBank™

AF080214) primers were 5′-CAGTTTGGGTCTGAATTGTGTCG-3′, 5′-TGCACGAGCTTATGCTGCTGAC-3′, 5′-TGGATGAGTTTTCTGCATCTGTCC-3′, 5′-CGTGATGTTCAGGGCAGGAATG-3′, 5′-TCCCCTTTTCTGCCTTGGAAG-3′, 5′-AAACTGTTGCCCACACCAGTCCAC-3′, 5′-AACCTCTATGGTGCCTACGTGC-3′, and 5′-CCAAGCCCAGCTAATTTTTG-3′, respectively. Amplified products were sequenced at the UNC Genome Analysis Facility.

Semi-quantitative PCR was performed in a LightCycler PCR machine® thermal cycler (10 min/95 °C; 5 s/55 °C, 8 s/72 °C; 45 cycles), using the LightCycler Fast start DNA master SYBER Green I kit (Roche Applied Science). Melting curve analysis was performed by heating the reactions from 65 °C to 95 °C at 0.11 °C intervals, and a fluorescence threshold (C_t) was determined using the LightCycler Software (version 4.0). C_t values were adjusted for differences in amplification efficiencies. Glyceraldehyde-3-phosphate dehydrogenase served as a housekeeping gene for normalization between samples and was included in each cycling run. The melting temperature of the PCR product for each reaction was monitored to ensure that only a single product of the correct size was amplified. Primer pairs for PAR3 were as above. Primers for glyceraldehyde-3-phosphate dehydrogenase were 5′-GAAGTTGAAGGTCGGAGTCA-3′ and 5′-GATCTCGCTCCTGGAAGATG-3′. The average crossover point was determined using the Roche Applied Science software. The relative expression levels of PAR3 were calculated from the efficiency of the PCR reaction and the crossing point, and normalized to the expression of the reference gene, as previously described (33).

Overexpression of PAR3 and Dominant Negative Mutants of RhoGEF and RhoA—A549 cells were transfected with pcDNA3.1 empty vector, pmaxFP-Green-C GFP-expressing vector, or vector containing the desired insert, using FuGENE HD (Roche Applied Science). pcDNA3.1 vectors expressing p115RGS and RhoA(T19N), and pBJ1 vector expressing HA-tagged PAR3, were kindly provided by Dr. T. K. Harden (34, 35) and Dr. S. R. Coughlin (36), respectively. A transfection efficiency of 70–80% was achieved, as assessed with the green fluorescent protein-expressing pmaxFP-Green-C vector.

Small Interference RNA (siRNA)—Oligonucleotides targeting human PAR3 and scrambled control (5′-GGCATTCTTTGGATTCTTA-3′ and 5′-GTGAGTTCGTTCTCTATTA-3′, respectively) were purchased from Dharmacon, Inc. A549 cells were transfected with 1 μg of oligonucleotide, using the Amaxa Nucleofector Device™ and Cell Line Nucleofector® Kit T (Amaxa Biosystems, Gaithersburg, MD), following the manufacturer's instructions. Transfected cells were grown in serum-supplemented Dulbecco's modified Eagle's medium for at least 24 h, prior to assays.

Site-directed Mutagenesis of PAR3—The QuikChange II XL® site-directed mutagenesis kit (Stratagene, La Jolla, CA) was used to generate a PAR3 mutant isoform ($PAR3^{196}$) resistant to siRNA oligonucleotide knockdown. The sequence 5′-GGCATTCTTTGGATTCTTA-3′ was mutated to 5′-GGCATTTTTTGGGTTCTTA-3′. Nucleotide changes and sequence integrity of the expression vector were confirmed by sequencing. A549 cells were cotransfected with a pBJ1 expression vector bearing $PAR3^{196}$ (100 ng) and the indicated siRNA oligonucleotide, using the Amaxa system, as described above.

RhoA Pulldown Assay—Measurements of GTP-bound RhoA were performed using the Rho Activation Assay Biochem Kit (Rhoketin assay), according to the manufacturer's instructions. Cell lysates and pulldown assays were resolved by SDS-PAGE and transferred to polyvinylidene difluoride membranes. RhoA was detected by Western blot, using monoclonal anti-RhoA antibody (1:500) provided by the manufacturer and IRdye®800-conjugated affinity-purified goat anti-mouse IgG (Rockland Immunochemicals, Philadelphia, PA). Immunoblots were revealed and quantified using the Odissey® Infrared Imaging System (LI-COR Biosciences, Lincoln, NE).

Myosin Light Chain Phosphorylation—Proteins were resolved by SDS-PAGE, and duplicated membranes were separately blotted with anti-phospho-MLC(Ser-19) antibody (1:500) or anti-MLC (1:1000) antibodies (Cell Signaling Technology Inc., Danvers, MA) by goat anti-rabbit Alexa Fluor® 680 secondary antibody (Invitrogen). Blots were quantified as indicated above.

Uptake of Propidium Iodide—Cells were rinsed and challenged with agonist for 5 min, in the presence of 20 μM propidium iodide. At the end of the incubation, the bathing solution was replaced with HBSS+ containing 4% paraformaldehyde. Confocal images of nuclear staining and differential interference contrast were acquired in a Leica SP5 confocal microscope, using a 561 nm laser and a 20× lens (Leica, Germany). The number of nuclei stained with propidium iodide was calculated using Adobe Photoshop.

Data Analysis—Differences between means were determined by unpaired Student's *t* test and were considered significant when $p < 0.05$.

RESULTS

Thrombin Promotes ATP Release from A549 Cells—The paucity of pharmacological approaches to trigger regulated nucleotide release poses a problem for studying the mechanism of ATP release from lung epithelial cells. Quantification of ATP release is further complicated by the presence of cell surface ecto-ATPases that rapidly hydrolyze released ATP. By implementing a protocol that quantifies ATP release in real-time in a thin film near the cell surface (28), we investigated the action of GPCR agonists on ATP release from lung epithelial cells.

Our initial screening revealed that the serine protease thrombin promoted robust ATP release from lung carcinoma A549 cells (Fig. 1). However, thrombin-evoked ATP release was evident only when ATP hydrolysis was inhibited. That is, in the absence of drugs, ATP levels on resting cells stabilized around $\sim 9 \pm 2$ nM and reached a level of 12 ± 4 nM after the addition of thrombin (30 nM, 10 min). In contrast, in the presence of ecto-ATPase inhibitors (30 μM ebselen and 300 μM β,γ-metATP (28)), extracellular ATP levels on resting cells increased modestly to 22 ± 7 nM in 10 min, likely reflecting constitutive nucleotide release (24, 28, 29). Addition of thrombin in the presence of ebselen and β,γ-metATP resulted in a robust increase of extracellular ATP, which reached a concentration of 113 ± 15 nM after 10 min (Fig. 1*A*). Based on these results, subsequent measurements of agonist-promoted ATP release were per-

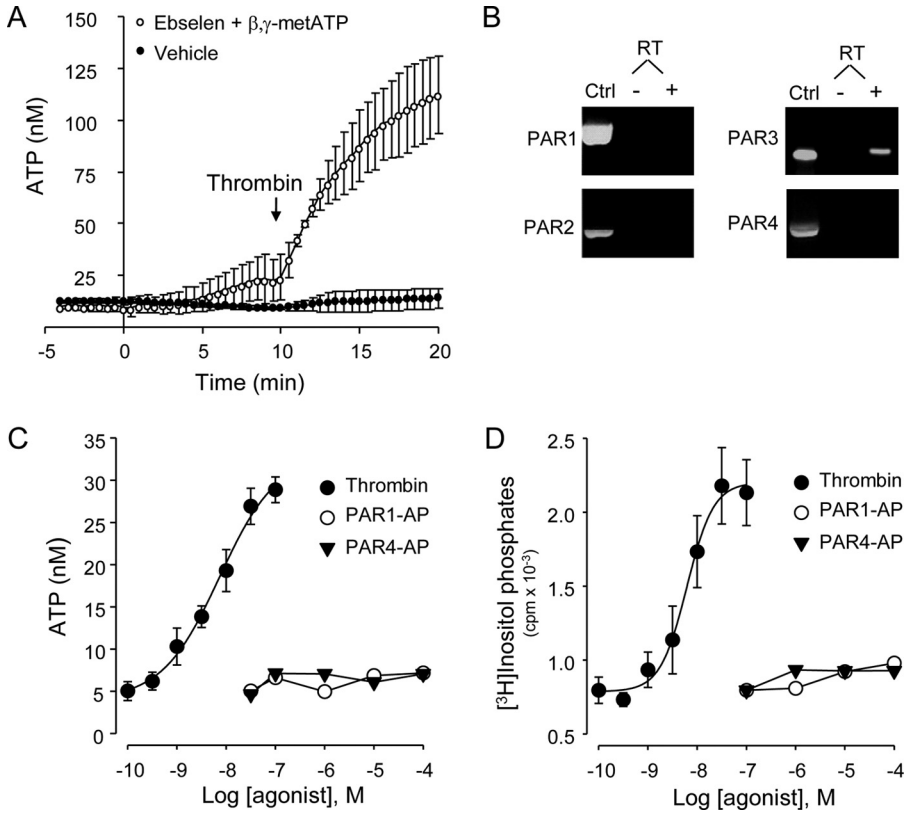

FIGURE 1. **Thrombin-promoted ATP release and inositol phosphate formation in a PAR1- and PAR4-independnet manner.** *A*, extracellular ATP concentrations were measured in real-time, in the absence or presence of 30 μM ebselen and 300 μM $\beta\gamma$-metATP (added at $t = 0$), as described under "Experimental Procedures." Thrombin (30 nM) was added at $t = 10$ min. Values are the mean ± S.E. of eight independent measurements. *B*, PAR mRNA expression in A549 cells was determined by RT-PCR analysis. Plasmids expressing the indicated PAR were used as positive controls (*Ctrl*). Results are representative of nine independent A549 cell RNA preparations. *C*, cells were stimulated for 5 min with thrombin, PAR1AP, or PAR4AP, and extracellular ATP measured was off-line, as described under "Experimental Procedures." Values are the mean ± S.E. of three independent measurements performed in sextuplicate. *D*, *myo*-[^{3}H]inositol-labeled cells were incubated for 20 min with the indicated agonist, and the resulting [^{3}H]inositol phosphates were separated and quantified, as described under "Experimental Procedures." Results are from three independent experiments performed with quadruplicate samples.

formed in the presence of 30 μM ebselen and 300 μM β,γ-metATP.

PAR3 Mediates Thrombin-promoted ATP Release in A549 Cells—Thrombin and other serine-proteases activate a family of four G protein-coupled receptors, referred as to protease-activated receptors (PAR1–PAR4). Thrombin activates PAR1, PAR3, and PAR4. The remaining member of the PAR family, PAR2, is activated by trypsin and other proteases but not by thrombin (reviewed in Refs. 37, 38). To gain an insight into the PAR subtype(s) present in A549 cells, RT-PCR studies were conducted. Fig. 1*B* illustrates that PAR3 but not PAR1, PAR2, or PAR4 transcripts could be amplified from A549 cells.

PARs are activated by proteolytic cleavage of the N-terminal exodomain of the receptor. This cleavage generates a new N terminus that functions as a tethered ligand, which binds to the body of the receptor and promotes signaling (37, 38). Synthetic peptides representing the newly formed N terminus selectively activate PAR1, PAR2, and PAR4, independent of receptor cleavage. Human PAR3 is not activated by PAR3-mimicking peptides, which suggests that PAR3 activation requires proteolytic cleavage at the N-terminal exodomain (36). Fig. 1*C* shows that thrombin, but not PAR1- and PAR4-activating peptides (PAR1AP and PAR4AP, respectively), elicited ATP release in a concentration-dependent manner. Enhanced ATP release was readily observed in response to 1 nM thrombin and was maximal with 30 nM thrombin ($EC_{50} = 7$ nM).

Because activation of thrombin receptors results in phospholipase C activation (36, 39, 40), we investigated the effect of thrombin and PAR-activating peptides on inositol phosphate formation, using [^{3}H]inositol-labeled A549 cells. Fig. 1*D* shows that thrombin promoted [^{3}H]inositol phosphate formation with a potency ($EC_{50} = 6.3$ nM) similar to that observed for ATP release. PAR1AP or PAR4AP promoted negligible [^{3}H]inositol phosphate formation (Fig. 1*D*). Altogether, the data in Fig. 1 suggest that PAR3 in the only thrombin receptor present in A549 cells.

To more definitively assess the involvement of PAR3 in thrombin-elicited ATP release, the effect of PAR3 overexpression/suppression was examined. Overexpression of PAR3 conferred enhanced thrombin-elicited ATP release and inositol phosphate formation to A549 cells, relative to vector-transfected cells (Fig. 2). Gain in thrombin-promoted ATP release was noted in cells transfected with as low as 10 ng of PAR3 cDNA/well and was robust with 100–300 ng of cDNA/well (Fig. 2*A*). The potency of thrombin in eliciting ATP release and inositol phosphate formation increased by ~5-fold ($EC_{50} = 1.1$ nM) and ~7-fold ($EC_{50} = 1.2$ nM), respectively, in cells transfected with 100 ng PAR3 cDNA, relative to vector-transfected cells (Fig. 2, *B* and *C*).

The contribution of PAR3 to ATP release from A549 cells was directly examined by targeting the endogenous PAR3 via siRNA. Transfection of A549 cells with a PAR3-selective (but not its scramble) siRNA oligonucleotide resulted in ~60% decrease of PAR3 transcripts, as judged by quantitative PCR (Fig. 3*A*). This manipulation also resulted in ~50% inhibition of thrombin-evoked inositol phosphate formation (Fig. 3*B*) and ATP release (Fig. 3*C*). The PAR3 siRNA approach had no effect on GPCR (other than PAR3)-mediated signaling, because UTP-evoked inositol phosphate formation was unaffected in PAR3 siRNA-transfected cells (vehicle, 1155 ± 178 cpm; UTP, 5430 ± 177 cpm; PAR siRNA-transfected cells: vehicle, 1195 ± 164 cpm; UTP, 5869 ± 257 cpm; mean ± S.D., $n = 4$). To verify that the siRNA approach did not knock down downstream effectors of PAR3, cells were cotransfected with PAR3^{196}, a

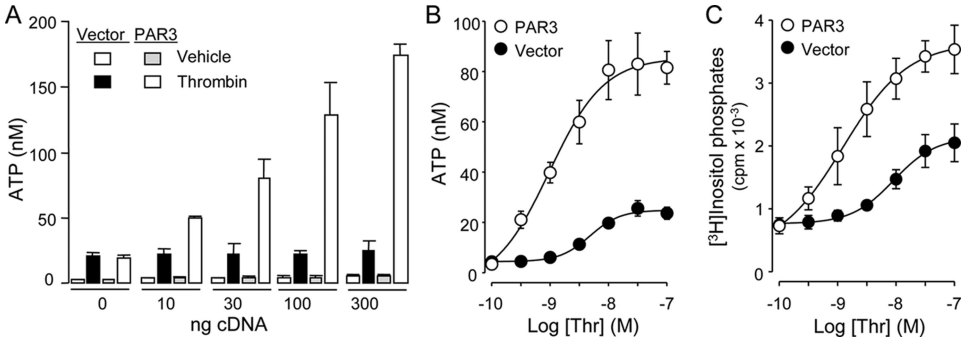

FIGURE 2. **PAR3 overexpression enhances thrombin-elicited ATP release and inositol phosphate formation in A549 cells.** *A*, cells were transfected with the indicated amount of cDNA. Forty-eight hours post transfection, cells were preincubated with ebselen and $\beta\gamma$-metATP as in Fig. 1 and incubated for 5 min with 30 nM thrombin or vehicle. *B* and *C*, cells transfected with 100 ng of PAR3 cDNA were stimulated for 5 min (*B*) or 20 min (*C*) with the indicated concentration of thrombin, and ATP release and inositol phosphate formation were measured as described in Fig. 1, *C* and *D*, respectively. The data represent the mean ± S.E. of at least three independent experiments performed in quadruplicate.

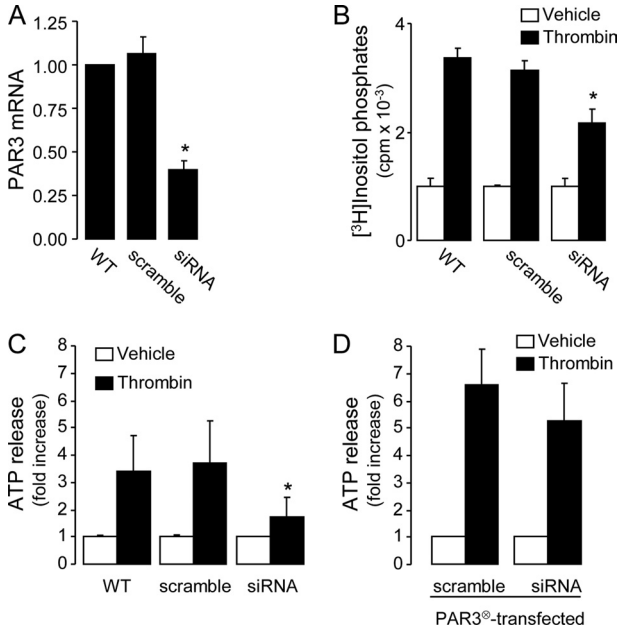

FIGURE 3. **PAR3 mediates thrombin-elicited ATP release and inositol phosphate formation in A549 cells.** *A*, PAR siRNA reduces PAR3 mRNA expression. *B*, effect of PAR3 siRNA on thrombin (30 nM)-promoted inositol phosphate formation. *C*, ATP release was measured in cells transfected with either PAR3 siRNA or its scramble oligonucleotide. *D*, cells transfected as above were cotransfected with empty-vector or siRNA-resistant $PAR3^{196}$ cDNA ($PAR3^{\otimes}$). ATP was measured off-line, 5 min after the addition of vehicle or 30 nM thrombin, in the presence of 30 μM ebselen and 300 μM $\beta\gamma$-metATP. The data represent the mean ± S.E. of three separate experiments performed in triplicate; $p < 0.05$.

PAR3 cDNA mutant resistant to the PAR3 siRNA oligonucleotide. $PAR3^{196}$-mediated ATP release was not affected by PAR3 siRNA (Fig. 3*D*). Altogether, these results indicate that PAR3 is the major contributor to thrombin-evoked ATP release in A549 cells.

Ca^{2+} Is Necessary but Not Sufficient for Agonist-evoked ATP Release—Cytosolic Ca^{2+} is an important regulator of ATP release in many cells. For example, in excitatory tissues, ATP is released from ATP storage granules via Ca^{2+}-regulated exocytosis (20). Ca^{2+}-dependent ATP release has been also reported in cells lacking specialized ATP storage granules (21–23, 25, 41). Preincubation of A549 cells with 10 μM BAPTA-AM or 1 μM thapsigargin resulted in major inhibition of thrombin-promoted ATP release (Fig. 4*A*), suggesting that Ca^{2+} is required for ATP release from thrombin-stimulated A549 cells.

Because thrombin-elicited ATP release requires a Ca^{2+}-dependent step, we asked whether Ca^{2+}-mobilizing receptors other than PARs (*e.g.* $P2Y_2$-R) promote ATP release from these cells. Incubation of A549 cells with 100 μM UTP resulted in enhanced extracellular ATP concentrations, but the effect of UTP on ATP levels was modest, relative to thrombin (Fig. 4*B*). To investigate whether differences in UTP- *versus* thrombin-elicited second messenger signaling have accounted for the observed differences in agonist-promoted ATP release, UTP-promoted phosphoinositide breakdown was examined. UTP promoted inositol phosphate formation responses that were greater than thrombin responses. Nucleotide-evoked inositol phosphate formation, with potency order UTP = ATP ≫ ADP, UDP, was consistent with $P2Y_2$-R expression (Fig. 4*C*). RT-PCR analysis confirmed the expression of $P2Y_2$-R transcripts in A549 cells (not shown). Importantly, UTP promoted Ca^{2+} mobilization responses in Fura-2-acetoxymethyl ester-loaded A549 cells that were similar or greater in magnitude than thrombin (Fig. 4*D*). Altogether, the results suggest that receptor-promoted G_q/phospholipase-β activation/Ca^{2+} mobilization alone was not sufficient to elicit ATP release from A549 cells.

Thrombin-induced ATP Release Is Independent of G_i Activation—It has been established that PAR1 interacts with G_q, G_i, and $G_{12/13}$ families of G proteins (37, 42). Unlike PAR1, the G protein coupling of PAR3 is poorly defined. The fact that thrombin promotes phosphoinositide breakdown in a PAR3-dependent manner in A549 cells (Figs. 2 and 3), as well as in PAR3-transfected COS-7 cells (36), suggests that PAR3 couples to G_q. However, as mentioned above, signaling in addition to G_q/phospholipase C/Ca^{2+} is likely involved in thrombin-evoked ATP release from A549 cells. To assess G_i activation in thrombin-stimulated A549 cells, thrombin-promoted inhibition of cAMP formation was examined. Addition of 30 μM forskolin (in the presence of the phosphodiesterase inhibitor 3-isobutyl-1-methylxanthine) markedly enhanced cAMP formation in A549 cells (control, 8 ± 2 pmol/well; forskolin, 103 ± 6 pmol/well), which was inhibited (27% maximal inhibition) by thrombin, in a dose-dependent manner (supplemental Fig. S1*A*). Pertussis toxin, which ADP-ribosylates and inhibits $G_{\alpha i}$ proteins, reversed the inhibitory effect of thrombin on forskolin-elicited cAMP formation (supplemental Fig. S1*A*). Pertussis toxin failed to inhibit thrombin-promoted ATP release (supplemental Fig. S1*B*). Thus, although these results illustrated the presence of a G_i-coupled thrombin receptor in A549 cells, ATP release was not regulated by G_i activation. Consistent with these results, preincubation of cells with the phosphatidylinositol 3-kinase inhibitor wortmannin (200 nM/15 min) had no

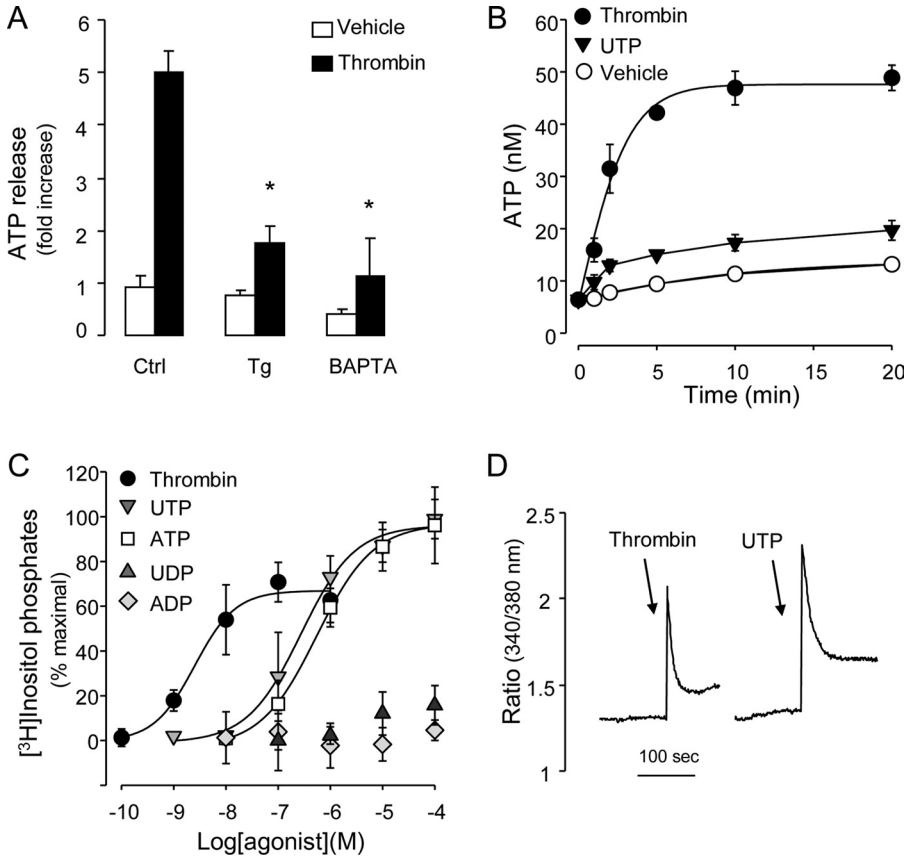

FIGURE 4. **Ca^{2+} is necessary but not sufficient for agonist-evoked ATP release.** *A*, cells were preincubated for 20 min with vehicle (*Ctrl*), 1 μM thapsigargin (*Tg*), or 10 μM BAPTA-AM (*BAPTA*), and ATP concentrations were measured off-line, 5 min following the addition of vehicle or 30 nM thrombin. Ebselen (30 μM) and $\beta\gamma$-metATP (300 μM) were added to cells 5–10 min prior addition of vehicle/thrombin. The data represent the mean ± S.E. of at least six separate experiments performed in quadruplicate. *B*, cells were incubated with vehicle, 30 nM thrombin, or 100 μM UTP, and ATP concentrations were measured as above. *C*, *myo*-[^{3}H]inositol-labeled cells were incubated for 20 min with the indicated drugs, and the resulting [^{3}H]inositol phosphates were separated and quantified as in Fig. 1*D*. Results are from four independent experiments performed with quadruplicate samples. *D*, cells were loaded with Fura-2-acetoxymethyl ester for 30 min and stimulated with 30 μM thrombin or 100 μM UTP. Fluorescence from 30–40 cells was acquired as described under "Experimental Procedures." Representative tracings are illustrated; similar results were obtained in six independent experiments.

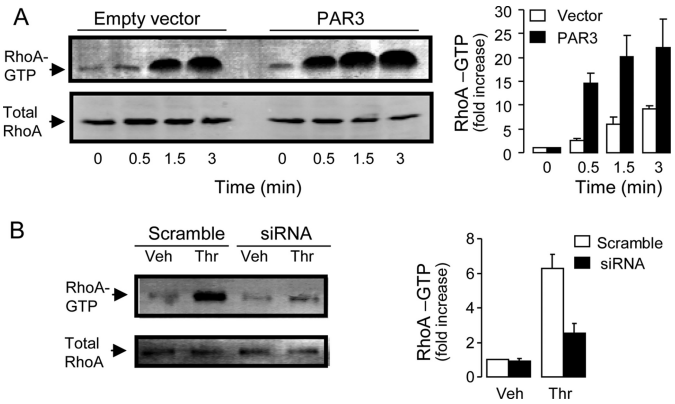

FIGURE 5. **PAR3 promotes RhoA activation.** *A*, total RhoA and RhoA-GTP were measured in A549 cells transfected with 100 ng of empty vector or PAR3 cDNA, as in Fig. 2. RhoA activation was visualized by the pulldown assay (*left*), as described under "Experimental Procedures." RhoA activation is expressed as -fold increase over control (vector, $t = 0$); values are the mean ± S.E. of ten independent experiments (*right*). *B*, PAR3 siRNA reduced thrombin (30 nM, 5 min)-promoted RhoA activation. The Western blot (*left*) is representative of four experiments performed under similar conditions. Values (*right*) are expressed as -fold increase over vehicle in scramble-transfected cells (mean ± difference to mean, $n = 4$).

effect on thrombin-elicited ATP release (supplemental Fig. S1*B*). Thus, phosphatidylinositol 3-kinase, known to be activated by β/γ subunits of G_i proteins downstream of PAR activation (43), was not involved in thrombin-promoted ATP release in A549 cells.

Thrombin Promotes ATP Release via $G_{12/13}$-mediated RhoGEF/RhoA Activation—Rho GTPases are well known downstream effectors of $G_{12/13}$, via $G_{\alpha 12/13}$ activation of guanine nucleotide exchange factors (GEFs) of Rho (RhoGEF) (reviewed in Ref. 44). Addition of thrombin to A549 cells caused a rapid and robust activation of RhoA, measured by the RhoA pulldown assay. RhoA activation was observed as early as 30 s post-thrombin addition and was robust after 90 s (Fig. 5*A*). Thrombin-elicited RhoA activation increased considerably in cells transfected with PAR3 (Fig. 5*A*) and was reduced by PAR3 siRNA (Fig. 5*B*).

To examine the possibility that PAR3-elicited ATP release involved activation of $G_{12/13}$/RhoGEF/Rho, A549 cells were transfected with dominant negative mutants of RhoGEF and RhoA. Transfection of A549 cells with p115RGS, a $G_{12/13}$-inhibitory protein derived from the RGS domain of p115-RhoGEF (34), impaired thrombin-promoted ATP release (Fig. 6*A*). Similarly, transfection of cells with the RhoA mutant RhoA(T19N), which tightly binds to RhoGEF but does not promote downstream effector activation (45), markedly inhibited thrombin-elicited ATP release (Fig. 6*A*). Control experiments indicated that thrombin-promoted inositol phosphate formation was not significantly affected by p115RGS or RhoA(T19N) transfections (Table 1).

Rho kinases (ROCKs) are important effectors of Rho (46). Preincubation of A549 cells with the ROCK inhibitor Y27632 resulted in dose-dependent inhibition of thrombin-promoted ATP release, with maximal inhibition observed with 1 μM Y27632 (Fig. 6, *B* and *D*). H1152, a more potent and selective ROCK inhibitor than Y27632 (47), also reduced ATP release in response to thrombin (Fig. 6*B*). ROCK activation is known to promote MLC phosphorylation, *e.g.* by phosphorylating and inactivating MLC phosphatase (48). Consistent with the possibility that MLC is an effector of ROCK upstream of ATP release, thrombin-promoted MLC phosphorylation was observed and was inhibited by 100 nM H1152 (Fig. 6*C*). Further, ML-7 (1 μM), an inhibitor of the Ca^{2+}/calmodulin-dependent MLC kinase (MLCK) (49), reduced MLC phospho-

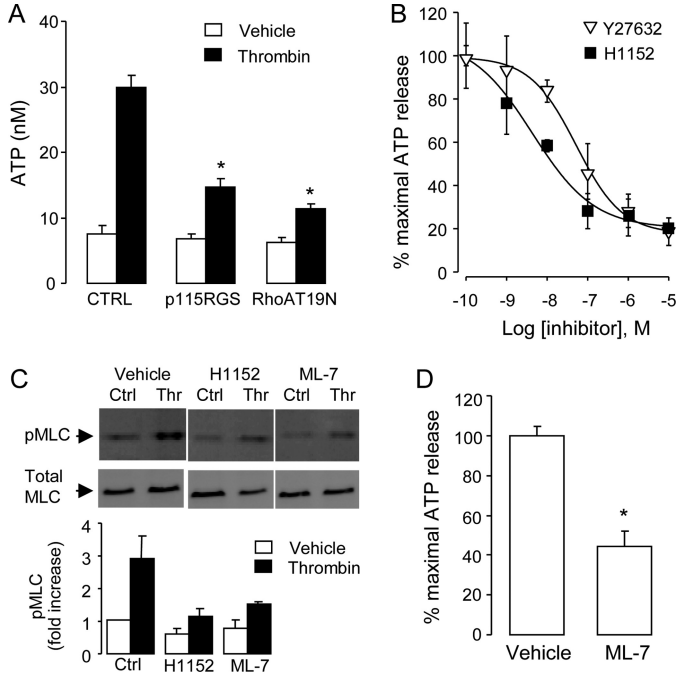

FIGURE 6. **Thrombin-elicited ATP release is mediated by $G_{12/13}$/RhoA/ROCK.** *A*, ATP release was quantified in P115-RGS-, or RhoA(T19N)- transfected cells, after 5-min incubation with 30 nM thrombin or vehicle. Values are the mean ± S.E. of four independent experiments performed in quadruplicate. *B*, cells were preincubated for 1 h with the indicated concentrations of H1152 or Y27632, and ATP release was measured after 5-min incubation with 30 nM thrombin or vehicle. The data are plotted as the percent of stimulation observed with 30 nM thrombin, in the absence of inhibitors. Values the mean ± S.E. from five separate experiments performed in quadruplicate. *C*, the effect of 100 nM H1152 or 1 μM ML-7 on thrombin-promoted MLC phosphorylation is illustrated by a Western blot (*top*). Quantification of p-MLC is indicated in the *bottom*; mean ± S.D., $n = 3$. *D*, effect of 1 μM ML-7 on thrombin-promoted ATP release. Values are the mean ± S.D. from at least three independent experiments performed in quadruplicate. *, significant inhibition of thrombin responses, $p < 0.05$. ATP measurements were performed in the presence of ebselen and $\beta\gamma$-metATP as indicated in previous figures.

TABLE 1

Thrombin-promoted inositol phosphate formation is not affected by Ca^{2+}, Rho, or connexin/pannexin inhibitors

myo-[^{3}H]Inositol-labeled A549 cells were challenged for 20 min with 30 nM thrombin, and the resulting inositol phosphates were quantified as indicated under "Experimental Procedures." Transfections and preincubations with pharmacological inhibitors were as in Fig. 8.

	Inhibitor	Mean ± S.D.	*n*
		cpm	
Control		1638 ± 296	8
Thrombin		3187 ± 516	8
Thrombin	P115-RGS	3516 ± 251	4
Thrombin	RhoA(T19N)	2680 ± 82	4
Thrombin	1 μM H1152	3536 ± 496	8
Thrombin	10 μM Y27632	3269 ± 202	8
Thrombin	1 μM ML-7	2924 ± 227	4
Thrombin	100 μM Anandamide	3361 ± 235	4
Thrombin	100 μM Flufenamic Acid	3076 ± 467	4
Thrombin	10 μM Carbenoxolone	3316 ± 289	8

rylation (Fig. 6*C*) and impaired ATP release (Fig. 6*D*) in thrombin-stimulated A549 cells. None of these inhibitors affected the ability of thrombin to promote inositol phosphate formation (Table 1).

Altogether, these data illustrate that Rho activation is necessary for PAR3-promoted ATP release in A549 cells. The data also suggest that Rho actions are mediated, at least in part, by ROCK activation, likely facilitating MLC phosphorylation by MLCK.

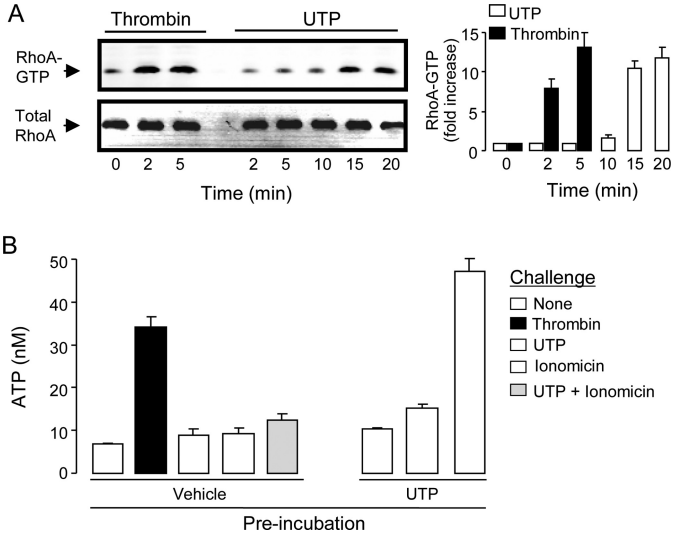

FIGURE 7. **RhoA activation and Ca^{2+} mobilization act in concert to promote ATP release.** *A*, RhoA activation was measured and quantified in A549 cells stimulated for the indicated times with 30 nM thrombin or 100 μM UTP. The results (-fold increase relative to untreated cells) represent the mean ± S.E. of five separate experiments. *B*, ATP release was measured in cells preincubated with vehicle or 100 μM UTP for 15 min, and challenged for additional 5 min with the indicated drugs. The data represent the mean ± S.E. of three separate experiments performed in quadruplicate. Ebselen and $\beta\gamma$-metATP were added as indicated in previous figures.

ATP Release Requires the Coordinated Action of Ca^{2+}- and Rho-dependent Pathways—Because $P2Y_2$-R stimulation has been linked to RhoA activation in endothelial cells (50), we asked whether UTP promotes RhoA activation in A549 cells and, if so, whether such activation differed from that of thrombin. Fig. 7*A* shows that incubation of A549 cells with 100 μM UTP resulted in RhoA activation that was similar in magnitude to thrombin. However, unlike the rapid effect of thrombin, UTP-promoted RhoA activation was observed only after 15 min. Thus, although thrombin promoted RhoA activation and Ca^{2+} mobilization (Figs. 4, 5, and 7) with overlapping time frames (30–90 s), UTP-induced RhoA activation was dissociated in time from Ca^{2+} responses (Figs. 4 and 7).

We hypothesized that Rho activation and Ca^{2+} mobilization must be temporally coordinated to promote ATP release. To assess this hypothesis, cells were preincubated for 15 min with 100 μM UTP (to achieve robust RhoA activation), followed by a 5-min challenge with the Ca^{2+} ionophore ionomycin. As a control, cells were preincubated with vehicle. Fig. 7*B* illustrates that addition of ionomycin (either alone or in combination with UTP) to untreated cells resulted in negligible ATP release. In contrast, addition of ionomycin to cells that were preincubated for 15 min with UTP resulted in robust release of ATP (Fig. 7*B*). The simplest interpretation of these results is that maximal ATP release requires synchronized activation of Rho and Ca^{2+} signaling.

Thrombin Promotes Opening of Connexin-like Hemichannels in a Ca^{2+} and ROCK-dependent Manner—Connexin and pannexin hemichannels have been proposed as a electrodiffusive pathway for the release of ATP under various experimental conditions (51, 52). Connexin (but not pannexin) hemichannels close at millimolar extracellular Ca^{2+} ($[Ca^{2+}]_{ex}$) and open when $[Ca^{2+}]_{ex}$ is lowered. Exposure to lowered extracellular

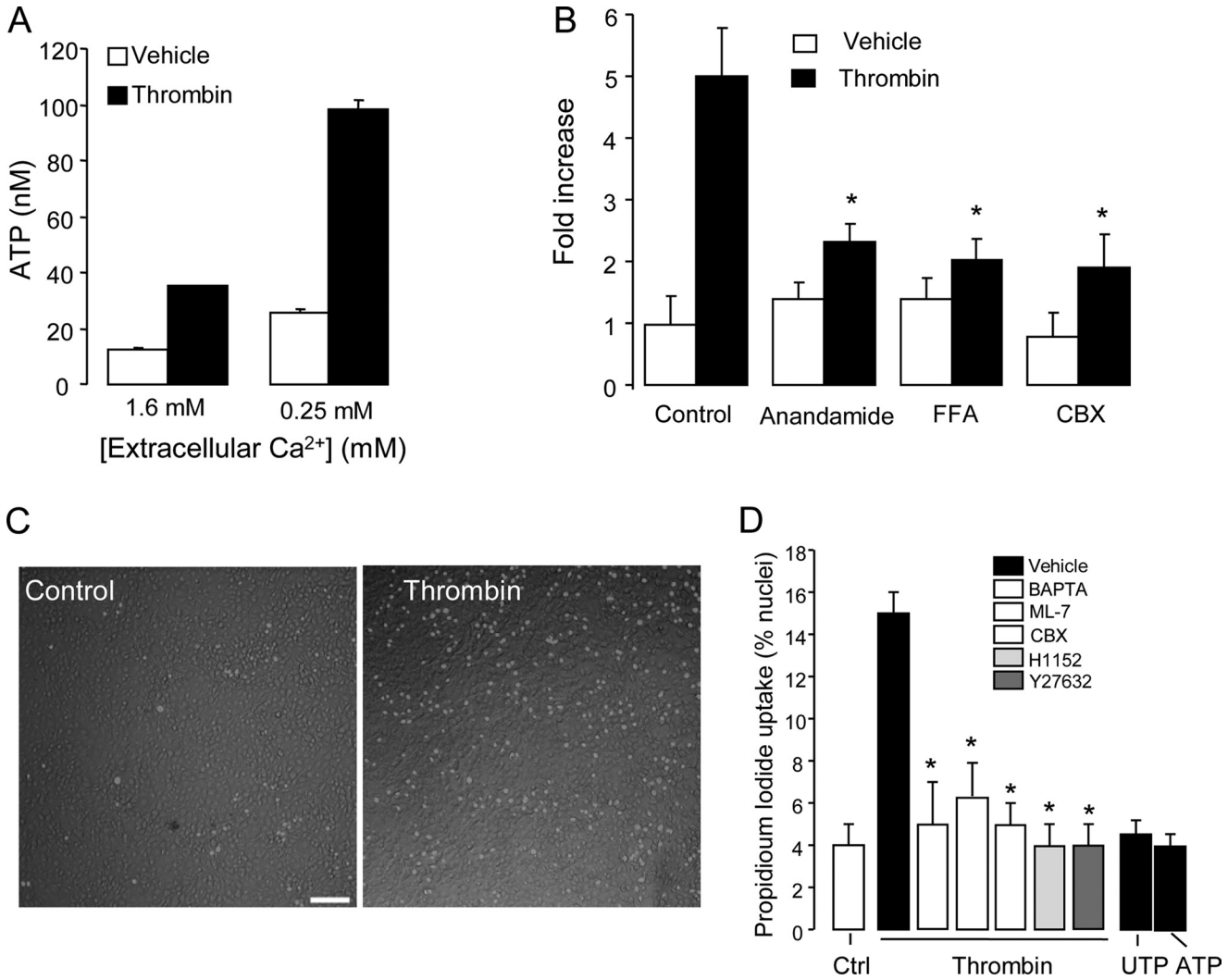

FIGURE 8. **Involvement of connexin/pannexin hemichannels in thrombin-promoted ATP release from A549 cells.** *A*, cells were preincubated for 2 min in EGTA/Ca^{2+}-buffered solutions, and extracellular ATP was measured after an additional 5-min incubation with vehicle or 30 nM thrombin. The data represent the mean ± S.E. of three separate experiments performed in quadruplicate. *B*, changes in ATP concentrations were measured in cells preincubated for 15 min with 100 μM arachidonylethanolamide, 100 μM flufenamic acid (*FFA*), or 10 μM carbenoxolone (*CBX*), and challenged for 5 min with vehicle or 30 nM thrombin. Values represent the mean ± S.E. of at least six separate experiments performed in quadruplicate. All ATP measurements were in the presence of 30 μM ebselen and 300 μM β,γ-metATP. *C*, uptake of cells with propidium iodide was assessed after 5-min incubation with vehicle or 30 μM thrombin. The images represent an overlay of propidium iodide (*red*)-associated nuclear fluorescence and differential interference contrast. *D*, A549 cells were preincubated with vehicle or with 10 μM carbenoxolone (*CBX*, 15 min), 10 μM Y27632 (45 min), 1 μM H1152 (45 min), 10 μM BAPTA-AM (20 min), or with 1 μM ML-7 (45 min), and challenged for 5 min with no agonist (*Ctrl*), 30 nM thrombin, 100 μM UTP, or 1 mM ATP in the presence of propidium iodide. Cells were fixed, and images were taken and analyzed by confocal microscopy. Dye uptake is expressed as the percent of nuclei displaying red fluorescence. The data are the mean ± S.E., $n = 4$. Similar results were obtained in at least three separate experiments performed in quadruplicate. Incubations in *B–D* were in HBSS+ containing 1.6 mM $CaCl_2$. *Bar*, 100 μm. *, significant inhibition of thrombin responses, $p < 0.05$.

divalent ion conditions is a well known procedure to potentiate or trigger the opening of connexin hemichannels, leading to ATP release (53, 54). In addition, both pannexins and connexins have been reported to conduct ATP at physiologically relevant $[Ca^{2+}]_{ex}$ (51, 52).

While investigating the role of calcium in PAR-stimulated responses, we observed that removal of $[Ca^{2+}]_{ex}$ resulted in enhanced ATP release from resting and thrombin-stimulated A549 cells (Fig. 8*A*), suggesting that connexin hemichannels are present on the A549 cell surface. This observation led us to investigate the possibility that hemichannels were involved in the release of ATP from thrombin-stimulated A549 cells, under normal $[Ca^{2+}]_{ex}$ conditions. Fig. 8*B* illustrates that thrombin-induced ATP release, assessed in the presence of 1.6 mM $[Ca^{2+}]_{ex}$, was markedly inhibited by non-selective connexin/pannexin inhibitors (100 μM arachidonylethanolamide, 100 μM flufenamic acid, and 10 μM carbenoxolone). Control experiments indicated that none of the hemichannel inhibitors affected thrombin-evoked inositol phosphate formation (Table 1).

To further assess the possibility that thrombin promoted connexin/pannexin hemichannel opening, the uptake of the hemichannel-permeable reporter dye propidium iodide was investigated. Propidium iodide displays low intrinsic fluorescence, but its fluorescence increases 20- to 30-fold upon binding to nucleic acids. Under resting conditions, a small population (<4%) of A549 cell nuclei were labeled with propidium iodide, but dye uptake increased markedly (3- to 4-fold) follow-

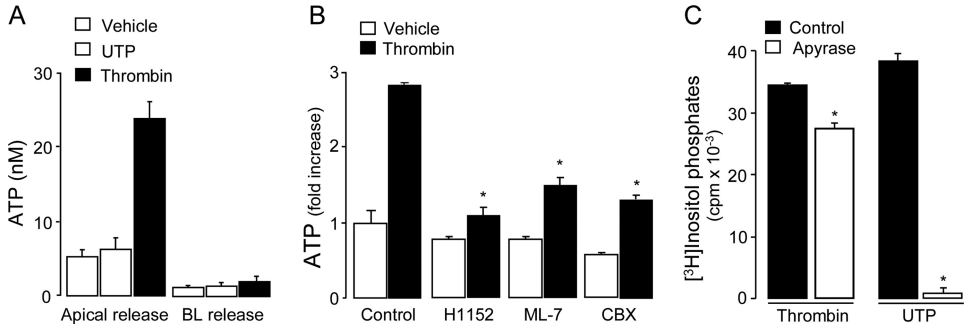

FIGURE 9. **Thrombin-promoted ATP release and inositol phosphate formation in primary HBE cells.** *A*, well differentiated primary HBE cells were incubated for 5 min with 30 nM thrombin (basolateral), 100 μM UTP (apical), or vehicle; ATP released to the apical or basolateral (*BL*) medium was quantified, as indicated under "Experimental Procedures." *B*, HBE cells were preincubated bilaterally (1 h) with 1 μM H1152, 10 μM ML-7 or1 μM CBX, and apical ATP release was measured after 5-min incubation with 30 nM thrombin (basolateral addition) or vehicle. *C*, [^{3}H]inositol-labeled HBE cells were incubated for 20 min in the presence of vehicle, 30 nM thrombin (basolateral addition), 100 μM UTP (apical addition), and in the absence or presence of 5 U/ml apyrase (apical addition). The resulting [^{3}H]inositol phosphates were quantified as indicated under "Experimental Procedures." The data (mean $\pm$ S.D.) represent the net increase in counts above background, and they are representative of two separate experiments with independent cultures performed each with quadruplicate samples. *, indicates significant difference between apyrase-treated *versus* non-treated cultures, $p < 0.01$.

ing a 5-min incubation of the cells with 30 nM thrombin (Fig. 8*C*). Unlike propidium iodide, which has a relatively small molecular mass (668.4 Da), the endocytosis marker fluorescein Dextran (3000–10000 Da) was not taken up by thrombin-stimulated A549 cells (not shown). Consistent with connexin/pannexin hemichannel involvement in agonist-promoted dye uptake, carbenoxolone inhibited the effect of thrombin on nucleus-associated fluorescence (Fig. 8*D*). Particularly relevant to our present study was the observation that thrombin-induced dye uptake was markedly inhibited by ROCK (Y26632 and H1152) or MLCK inhibitors (ML-7), and BAPTA-AM (Fig. 8*D*). Unlike thrombin, UTP (100 μM) and ATP (1 mM) promoted no changes in dye uptake (Fig. 8*D*), indicating that $P2Y_2$-R activation did not suffice to induce hemichannel opening. Moreover, lack of effect of 1 mM ATP on propidium iodide uptake argues against the possibility that the pore forming $P2X_7$-R (55) is expressed in these cells. Altogether, these data suggest that thrombin promoted Ca^{2+}- and Rho-regulated ATP release via connexin/pannexin hemichannels in A549 cells.

Thrombin Promotes Mucosal ATP Release from Primary Cultures of Well Differentiated HBE Cells—Having identified mechanistic components involved in ATP release in A549 cells, we asked whether observations made with these cells apply to physiologically relevant airway epithelia. Therefore, we examined the effect of thrombin on ATP release from polarized cultures of well differentiated primary HBE cells. Addition of 30 nM thrombin to the mucosal compartment had no effect on ATP release (not shown). In contrast, thrombin added to the basolateral compartment of HBE cultures resulted in a robust release of ATP through the apical (but not basolateral) surface (Fig. 9*A*). These data are in agreement with previous observations indicating that (i) ATP release occurs through elements that segregate to the apical domain after cell polarization (1, 33), and (ii) PARs are expressed at the basolateral membrane of polarized lung epithelial cells (56–58). The identity of the PAR evoking ATP release in primary HBE cells remains to be elucidated. As in A549 cells, the effect of thrombin on ATP release was markedly reduced in HBE cells that were preincubated with the ROCK inhibitor H1152, the MLCK inhibitor ML-7, or the connexin/pannexin hemichannel blocker carbenoxolone (Fig. 9*B*). Unlike thrombin, mucosal UTP caused no ATP release from HBE cells (Fig. 9*A*), despite the well established presence of $P2Y_2$ receptors on these cells (59, 60) (see Fig. 9*C*).

Regardless the lack of effect of UTP on ATP release (Fig. 9*A*), the presence of phospholipase C-activating $P2Y_2$ receptors on the apical surface of HBE cells (59, 60) suggests that ATP released onto the thin liquid film covering the mucosal airway epithelial cell surface contributed, at least in part, to PAR-evoked signaling. To test this possibility, the effect of the ATPase enzyme apyrase on thrombin-elicited [^{3}H]inositol phosphate formation was assessed. To minimize dilution of released ATP, the mucosal surface liquid volume was reduced to 100 μl/well (83 μl/cm^2 culture). Inclusion of 5 units of apyrase in this thin airway surface liquid resulted in small (21%) but reproducible decrease of [^{3}H]inositol phosphate formation in response to basolateral addition of thrombin (Fig. 9*C*). As expected, (mucosal) UTP promoted [^{3}H]inositol phosphate formation, which was nearly abolished in the presence of apyrase (Fig. 9*C*).

DISCUSSION

By examining the effects of PAR and P2Y-R agonists, we demonstrated that Rho/Rho kinases, in concert with cytosolic Ca^{2+}, are important regulators of ATP release. We also demonstrated that connexin/pannexin hemichannels are likely effectors of Rho/ROCK and Ca^{2+} signaling pathways that mediate ATP release from lung epithelial cells. An additional novel finding was that thrombin actions on A549 cells are mediated by PAR3, a poorly characterized thrombin receptor subtype.

Our data, indicating that BAPTA and thapsigargin impaired ATP release from thrombin-stimulated A549 cells, are consistent with the notion that Ca^{2+} mobilization is necessary for ATP release. However, ATP release in response to Ca^{2+}-mobilizing agents (*e.g.* UTP and ionomycin) represented a minor fraction relative to that observed with thrombin stimulation (Fig. 4). Thrombin-promoted ATP release decreased in cells transfected with dominant negative mutants of p115-RhoGEF and RhoA as well as in cells exposed to ROCK inhibitors (Fig. 6). Thus, Rho GTPases are key regulators of PAR-elicited ATP release. Importantly, Rho activation itself promoted no ATP release when temporarily dissociated from Ca^{2+} mobilization. Therefore, Rho signaling is an obligatory partner of Ca^{2+} mobilization upstream of ATP release in A549 cells.

Our present results are also consistent with previous studies implicating Rho as modulator of ATP release. Ito and cowork-

ers illustrated that Y26632 impaired lysophosphatidic acid- and/or hypotonic challenge-promoted ATP release in human umbilical vein and bovine aortic endothelial cells (61, 62). In a recent report, Blum *et al.* (26) illustrated that inactivation of RhoGTPases with *Clostridium botulinum* C3 exoenzyme impaired thrombin- and lysophosphatidic acid-promoted Ca^{2+}-dependent ATP release from 1321N1 astrocytoma cells . However, Y26632 and ML-7 had no effect on ATP release in these cells, suggesting that Rho regulation of ATP release in 1321N1 astrocytoma cells occurred independently of ROCK and MLC phosphorylation. Unlike 1321N1 cells, Y26632, H1152, and ML-7 impaired thrombin-evoked ATP release in A549 cells. Although Rho activation may utilize downstream effectors in addition to ROCK (63), our results suggest that ROCK is an important regulator of ATP release from A549 cells. Moreover, our data suggest that Ca^{2+}- and Rho/ROCK-dependent ATP release from thrombin-stimulated A549 cells occurs via connexin or pannexin hemichannels, a pathway that appeared not competent for ATP release in 1321N1 astrocytoma cells (26). Specifically, in A549 cells: (i) thrombin-promoted ATP release was inhibited by connexin/pannexin inhibitors, (ii) thrombin promoted the uptake of propidium iodide, an indicator of non-selective pore opening, which was inhibited by connexin/pannexin inhibitors, and (iii) thrombin-elicited dye uptake was inhibited by ROCK and MLCK inhibitors and by BAPTA-AM.

Our study did not address the identity of the putative hemichannel involved in ATP release. Based on the effect of $[Ca^{2+}]_{ex}$, connexin hemichannels likely are expressed at the plasma membrane of A549 cells. However, whether a connexin or pannexin hemichannel was responsible for the release of ATP in physiologically relevant $[Ca^{2+}]_{ex}$, as well as the mechanism potentially involved in hemichannel activation, remain to be investigated.

A surprising finding in our study was that thrombin actions in A549 cells could not be associated with PAR1. Although we have recently reported that the PAR1 peptide TFLLRNPNDK promoted nucleotide release and inositol phosphate formation in 1321N1 human astrocytoma cells (25), TFLLRNPNDK failed to promote these responses in A549 cells. Moreover, A549 cells used in the current study do not express PAR1 transcripts (Fig. 1). Our data also suggest that PAR4 is not expressed in A549 cells (Fig. 1). The finding that thrombin actions on A549 cells were not mediated by PAR1 or PAR4 was striking, because the ability of PAR3 (the other member of the thrombin receptor family) to generate intracellular signaling has been questioned (36). The finding that murine PAR3 functions as a cofactor for proteolytic activation of PAR4 in platelets has reinforced the assumption that PAR3 does not signal by itself. However, this observation may also reflect cell type- and species-specific functions for distinct PARs (reviewed in Ref. 42). Expression of human PAR3 (but not empty vector) in COS-7 cells resulted in thrombin-evoked inositol phosphate formation (36), likely via G_q-mediated phospholipase C activation. In addition, co-expression of $G_{\alpha 16}$ (a G protein endogenously expressed in hematopoietic cells that promiscuously transduces GPCR activation into phospholipase C activation) also conferred enhanced and potent thrombin-promoted inositol phosphate formation to PAR3-transfected COS-7 cells (36).

Unlike other PARs, evidence that natively expressed PAR3 promotes cellular responses by its own is scarce. For example, Ostrowska and Reiser recently illustrated that thrombin, but not a PAR1 peptide, promoted interleukin-8 secretion from both lung epithelial and astrocytoma cells, and that silencing PAR1 and PAR3 simultaneously (but not PAR1 alone) resulted in reduced interleukin-8 production in astrocytoma cells. The authors suggested thrombin actions were mediated by PAR3 (64). McLaughlin *et al.* reported that thrombin-elicited transendothelial electrical resistance was mediated in part by PAR3, which (together with PAR1) is endogenously expressed in human endothelial cells. PAR3 suppression resulted in ~50% reduction of transendothelial electrical resistance, while PAR1 suppression completely reduced transendothelial electrical resistance in response to thrombin. Based on bioluminescent resonance energy transfer-2 measurements, the authors concluded that PAR3 dimerizes with and regulates PAR1 signaling (65). Our data, illustrating that (i) PAR1AP and PAR4AP fail to promote cellular responses in A549 cells, (ii) PAR3 is the only PAR transcript present in these cells, and (iii) PAR3 siRNA decreased thrombin-evoked responses, indicate that PAR3 is the major thrombin receptor functionally present in these cells. Moreover, the observation that PAR3 overexpression enhanced thrombin-elicited inositol phosphate formation, RhoA activation, and ATP release, strongly suggest that PAR3 is capable of triggering signaling. Collectively, our results demonstrate that thrombin actions on A549 cells are mediated by PAR3-promoted Ca^{2+} mobilization and Rho activation, and that these signaling cascades must be temporally coordinated to allow ATP release via connexin/pannexin hemichannel opening.

Key observations obtained with A549 cells were expanded to physiologically relevant primary cultures of well differentiated HBE cells. In these cultures, basolateral addition of thrombin resulted in robust mucosal ATP release, which was inhibited by ROCK and MLCK inhibitors as well as by connexin/pannexin hemichannel blockers (Fig. 9, *A* and *B*). In addition, measurements of [^{3}H]inositol phosphate formation in thrombin-stimulated HBE cells suggested a previously unnoticed autocrine action of released ATP, *i.e.* as a contributor to PAR-evoked signaling (Fig. 9*C*). In summary, our study is the first to demonstrate the occurrence of robust ATP release in GPCR agonist-stimulated human airway epithelial cells and to implicate the participation of ROCK and MLCK as potential upstream effectors of ATP release via connexin/pannexin hemichannels.

Acknowledgments—We thank Catja van Heusden and Dr. Carla Ribeiro for assistance during cAMP and Ca^{2+} measurements, respectively, and Dr. Robert Tarran for the use of the Leica SP5 confocal microscope system. We are indebted to Drs. Rafael García Mata and Keith Burridge for assistance during initial Rho pulldown assays and Dr. T. Ken Harden for useful comments. We thank Lisa Brown for editorial assistance with the manuscript.

REFERENCES

1. Lazarowski, E. R., Tarran, R., Grubb, B. R., van Heusden, C. A., Okada, S., and Boucher, R. C. (2004) *J. Biol. Chem.* **279,** 36855–36864
2. Tarran, R., Button, B., Picher, M., Paradiso, A. M., Ribeiro, C. M., Laz-

arowski, E. R., Zhang, L., Collins, P. L., Pickles, R. J., Fredberg, J. J., and Boucher, R. C. (2005) *J. Biol. Chem.* **280,** 35751–35759
3. Button, B., Picher, M., and Boucher, R. C. (2007) *J. Physiol.* **580,** 577–592
4. Davis, C. W., and Dickey, B. F. (2008) *Annu. Rev. Physiol.* **70,** 487–512
5. Morse, D. M., Smullen, J. L., and Davis, C. W. (2001) *Am. J. Physiol. Cell Physiol.* **280,** C1485–1497
6. Jia, Y., Mathews, C. J., and Hanrahan, J. W. (1997) *J. Biol. Chem.* **272,** 4978–4984
7. Devor, D. C., and Pilewski, J. M. (1999) *Am. J. Physiol.* **276,** C827–C837
8. Yue, G., Malik, B., Yue, G., and Eaton, D. C. (2002) *J. Biol. Chem.* **277,** 11965–11969
9. Ma, H. P., Saxena, S., and Warnock, D. G. (2002) *J. Biol. Chem.* **277,** 7641–7644
10. Kunzelmann, K., Bachhuber, T., Regeer, R., Markovich, D., Sun, J., and Schreiber, R. (2005) *FASEB J.* **19,** 142–143
11. Mason, S. J., Paradiso, A. M., and Boucher, R. C. (1991) *Br. J. Pharmacol.* **103,** 1649–1656
12. Cressman, V. L., Lazarowski, E., Homolya, L., Boucher, R. C., Koller, B. H., and Grubb, B. R. (1999) *J. Biol. Chem.* **274,** 26461–26468
13. Zsembery, A., Fortenberry, J. A., Liang, L., Bebok, Z., Tucker, T. A., Boyce, A. T., Braunstein, G. M., Welty, E., Bell, P. D., Sorscher, E. J., Clancy, J. P., and Schwiebert, E. M. (2004) *J. Biol. Chem.* **279,** 10720–10729
14. Boucher, R. C. (2002) *Adv. Drug Deliv. Rev.* **54,** 1359–1371
15. Rooney, S. A. (2001) *Comp. Biochem. Physiol. A Mol. Integr. Physiol.* **129,** 233–243
16. Factor, P., Mutlu, G. M., Chen, L., Mohameed, J., Akhmedov, A. T., Meng, F. J., Jilling, T., Lewis, E. R., Johnson, M. D., Xu, A., Kass, D., Martino, J. M., Bellmeyer, A., Albazi, J. S., Emala, C., Lee, H. T., Dobbs, L. G., and Matalon, S. (2007) *Proc. Natl. Acad. Sci. U.S.A.* **104,** 4083–4088
17. Blackburn, M. R., Lee, C. G., Young, H. W., Zhu, Z., Chunn, J. L., Kang, M. J., Banerjee, S. K., and Elias, J. A. (2003) *J. Clin. Invest.* **112,** 332–344
18. Sun, C. X., Zhong, H., Mohsenin, A., Morschl, E., Chunn, J. L., Molina, J. G., Belardinelli, L., Zeng, D., and Blackburn, M. R. (2006) *J. Clin. Invest.* **116,** 2173–2182
19. Picher, M., Burch, L. H., and Boucher, R. C. (2004) *J. Biol. Chem.* **279,** 20234–20241
20. Lazarowski, E. R., Boucher, R. C., and Harden, T. K. (2003) *Mol. Pharmacol.* **64,** 785–795
21. Boudreault, F., and Grygorczyk, R. (2004) *J. Physiol.* **561,** 499–513
22. Tatur, S., Groulx, N., Orlov, S. N., and Grygorczyk, R. (2007) *J. Physiol.* **584,** 419–435
23. Tatur, S., Kreda, S., Lazarowski, E., and Grygorczyk, R. (2008) *Purinergic. Signal.* **4,** 139–146
24. Joseph, S. M., Buchakjian, M. R., and Dubyak, G. R. (2003) *J. Biol. Chem.* **278,** 23331–23342
25. Kreda, S. M., Seminario-Vidal, L., Heusden, C., and Lazarowski, E. R. (2008) *Br. J. Pharmacol.* **153,** 1528–1537
26. Blum, A. E., Joseph, S. M., Przybylski, R. J., and Dubyak, G. R. (2008) *Am. J. Physiol. Cell Physiol.* **295,** C231–241
27. Asokananthan, N., Graham, P. T., Fink, J., Knight, D. A., Bakker, A. J., McWilliam, A. S., Thompson, P. J., and Stewart, G. A. (2002) *J. Immunol.* **168,** 3577–3585
28. Okada, S. F., Nicholas, R. A., Kreda, S. M., Lazarowski, E. R., and Boucher, R. C. (2006) *J. Biol. Chem.* **281,** 22992–23002
29. Lazarowski, E. R., Boucher, R. C., and Harden, T. K. (2000) *J. Biol. Chem.* **275,** 31061–31068
30. Fürstenau, C. R., Spier, A. P., Rücker, B., Luisa Berti, S., Battastini, A. M., and Sarkis, J. J. (2004) *Chem. Biol. Interact.* **148,** 93–99
31. Joseph, S. M., Pifer, M. A., Przybylski, R. J., and Dubyak, G. R. (2004) *Br. J. Pharmacol* **142,** 1002–1014
32. Lazarowski, E. R., Shea, D. A., Boucher, R. C., and Harden, T. K. (2003) *Mol. Pharmacol.* **63,** 1190–1197
33. Sesma, J. I., Esther, C. R., Jr., Kreda, S. M., Jones, L., O'Neal, W., Nishihara, S., Nicholas, R. A., and Lazarowski, E. R. (2009) *J. Biol. Chem.* **284,** 12572–12583
34. Hains, M. D., Siderovski, D. P., and Harden, T. K. (2004) *Methods Enzymol.* **389,** 71–88
35. Hains, M. D., Wing, M. R., Maddileti, S., Siderovski, D. P., and Harden, T. K. (2006) *Mol. Pharmacol.* **69,** 2068–2075
36. Ishihara, H., Connolly, A. J., Zeng, D., Kahn, M. L., Zheng, Y. W., Timmons, C., Tram, T., and Coughlin, S. R. (1997) *Nature* **386,** 502–506
37. Trejo, J. (2003) *J. Pharmacol. Exp. Ther.* **307,** 437–442
38. Steinhoff, M., Buddenkotte, J., Shpacovitch, V., Rattenholl, A., Moormann, C., Vergnolle, N., Luger, T. A., and Hollenberg, M. D. (2005) *Endocr. Rev.* **26,** 1–43
39. Hung, D. T., Wong, Y. H., Vu, T. K., and Coughlin, S. R. (1992) *J. Biol. Chem.* **267,** 20831–20834
40. Xu, W. F., Andersen, H., Whitmore, T. E., Presnell, S. R., Yee, D. P., Ching, A., Gilbert, T., Davie, E. W., and Foster, D. C. (1998) *Proc. Natl. Acad. Sci. U.S.A.* **95,** 6642–6646
41. Kreda, S. M., Okada, S. F., van Heusden, C. A., O'Neal, W., Gabriel, S., Abdullah, L., Davis, C. W., Boucher, R. C., and Lazarowski, E. R. (2007) *J. Physiol.* **584,** 245–259
42. Coughlin, S. R. (2000) *Nature* **407,** 258–264
43. Goel, R., Phillips-Mason, P. J., Gardner, A., Raben, D. M., and Baldassare, J. J. (2004) *J. Biol. Chem.* **279,** 6701–6710
44. Kurose, H. (2003) *Life Sci.* **74,** 155–161
45. Feig, L. A. (1999) *Nat. Cell Biol.* **1,** E25–E27
46. Schwartz, M. (2004) *J. Cell Sci.* **117,** 5457–5458
47. Davies, S. P., Reddy, H., Caivano, M., and Cohen, P. (2000) *Biochem. J.* **351,** 95–105
48. Riento, K., and Ridley, A. J. (2003) *Nat. Rev. Mol. Cell. Biol.* **4,** 446–456
49. Saitoh, M., Ishikawa, T., Matsushima, S., Naka, M., and Hidaka, H. (1987) *J. Biol. Chem.* **262,** 7796–7801
50. Seye, C. I., Yu, N., González, F. A., Erb, L., and Weisman, G. A. (2004) *J. Biol. Chem.* **279,** 35679–35686
51. Dahl, G., and Locovei, S. (2006) *IUBMB Life* **58,** 409–419
52. Goodenough, D. A., and Paul, D. L. (2003) *Nat. Rev. Mol. Cell. Biol.* **4,** 285–294
53. Stout, C. E., Costantin, J. L., Naus, C. C., and Charles, A. C. (2002) *J. Biol. Chem.* **277,** 10482–10488
54. De Vuyst, E., Decrock, E., Cabooter, L., Dubyak, G. R., Naus, C. C., Evans, W. H., and Leybaert, L. (2006) *EMBO J.* **25,** 34–44
55. Pelegrin, P., and Surprenant, A. (2006) *EMBO J.* **25,** 5071–5082
56. Danahay, H., Withey, L., Poll, C. T., van de Graaf, S. F., and Bridges, R. J. (2001) *Am. J. Physiol. Cell Physiol.* **280,** C1455–1464
57. Palmer, M. L., Lee, S. Y., Maniak, P. J., Carlson, D., Fahrenkrug, S. C., and O'Grady, S. M. (2006) *Am. J. Physiol. Cell Physiol.* **290,** C1189–C1198
58. Kunzelmann, K., Schreiber, R., König, J., and Mall, M. (2002) *Cell Biochem. Biophys.* **36,** 209–214
59. Paradiso, A. M., Mason, S. J., Lazarowski, E. R., and Boucher, R. C. (1995) *Nature* **377,** 643–646
60. Lazarowski, E. R., Paradiso, A. M., Watt, W. C., Harden, T. K., and Boucher, R. C. (1997) *Proc. Natl. Acad. Sci. U.S.A.* **94,** 2599–2603
61. Hirakawa, M., Oike, M., Karashima, Y., and Ito, Y. (2004) *J. Physiol.* **558,** 479–488
62. Koyama, T., Oike, M., and Ito, Y. (2001) *J. Physiol.* **532,** 759–769
63. Gavard, J., and Gutkind, J. S. (2008) *J. Biol. Chem.* **283,** 29888–29896
64. Ostrowska, E., and Reiser, G. (2008) *Cell Mol. Life Sci.* **65,** 970–981
65. McLaughlin, J. N., Patterson, M. M., and Malik, A. B. (2007) *Proc. Natl. Acad. Sci. U.S.A.* **104,** 5662–5667